

# Oxygen binding and activation by the complexes of PY2- and TPA-appended diphenylglycoluril receptors with copper and other metals†‡

Vera S. I. Sprakel,<sup>a</sup> Martin C. Feiters,<sup>\*a</sup> Wolfram Meyer-Klaucke,<sup>b</sup> Marten Klopstra,<sup>c</sup> Jelle Brinksma,<sup>c</sup> Ben L. Feringa,<sup>c</sup> Kenneth D. Karlin<sup>d</sup> and Roeland J. M. Nolte<sup>a</sup>

<sup>a</sup> Department of Organic Chemistry, Institute for Molecules and Materials, Radboud University Nijmegen, 1 Toernooiveld, NL-6525, ED Nijmegen, The Netherlands

<sup>b</sup> EMBL Outstation at DESY, Notkestrasse 85, D-22603, Hamburg, Germany

<sup>c</sup> Department of Organic and Molecular Inorganic Chemistry, Stratingh Institute, University of Groningen, Nijenborgh, NL-9747, AG Groningen, The Netherlands

<sup>d</sup> Department of Chemistry, The Johns Hopkins University, 3400 N. Charles Street, Baltimore, Maryland, 21218, USA

Received 5th May 2005, Accepted 20th June 2005

First published as an Advance Article on the web 23rd September 2005

The copper(I) complexes of diphenylglycoluril basket receptors **1** and **2**, appended with bis(2-ethylpyridine)amine (PY2) and tris(2-methylpyridine)amine (TPA), respectively, and their dioxygen adducts were studied with low-temperature UV-vis and X-ray absorption spectroscopy (XAS). The copper(I) complex of **1**, [**1**-Cu(I)<sub>2</sub>] or **1a**, forms a  $\mu$ - $\eta^2$ : $\eta^2$  dioxygen complex, whereas the copper(I) complex of **2**, [**2**-Cu(I)<sub>2</sub>] or **2a**, does not form a well defined dioxygen complex, but is oxidized to Cu(II). Dioxygen is bound irreversibly to **1a** and the formed complex is stable over time. The coordination geometries of the above complexes were determined by XAS, which revealed that pyridyl groups and amine N-donors participate in the coordination to Cu(I) ions in the complexes of both receptors. The catalytic activities of various metal complexes of **1** and **2**, that were designed as mimics of dinuclear copper enzymes that can activate dioxygen, were investigated. Phenolic substrates that were expected to undergo aromatic hydroxylation, showed oxidative polymerization without insertion of oxygen. The mechanism of this polymerization turns out to be a radical coupling reaction as was established by experiments with the model substrate 2,4-di-*tert*-butylphenol. In addition to Cu(II), the Mn(III) complex of **1** and the Fe(II) complex of **2** were tested as oxidation catalysts. Oxidation of catechol was observed for the Cu(II) complex of receptor **1** but the other metal complexes did not lead to oxidation.

## Introduction

In Nature, various dinuclear copper proteins exist that are able to bind oxygen, or activate it for reaction with a substrate. Hemocyanin, the oxygen-binding protein of arthropods and molluscs, binds molecular oxygen between two copper ions that are each coordinated by a set of three histidine-derived imidazole ligands.<sup>1–3</sup> The related enzymes, tyrosinase and catechol oxidase, are assumed to have oxygen binding sites similar to that of hemocyanin on the basis of comparable spectroscopic characteristics,<sup>4,5</sup> and the crystal structure of catechol oxidase<sup>6,7</sup> shows that the enzyme can be conceived as a metal-containing site for binding and activation of molecular oxygen, combined with a substrate binding site.

Taking the dinuclear copper enzymes as a source of inspiration for the development of new supramolecular catalysts as enzyme mimics, we have prepared new ligand appended receptors based on diphenylglycoluril baskets (Fig. 1), one (**1**) in which the PY2 (bis(2-ethylpyridine)amine) ligand was linked to the basket by a butyl spacer, and another (**2**) in which a TPA (tris(2-methylpyridine)amine) ligand is appended.<sup>8</sup> Interestingly, the bis-Cu(I) complex of a diphenylglycoluril basket that was

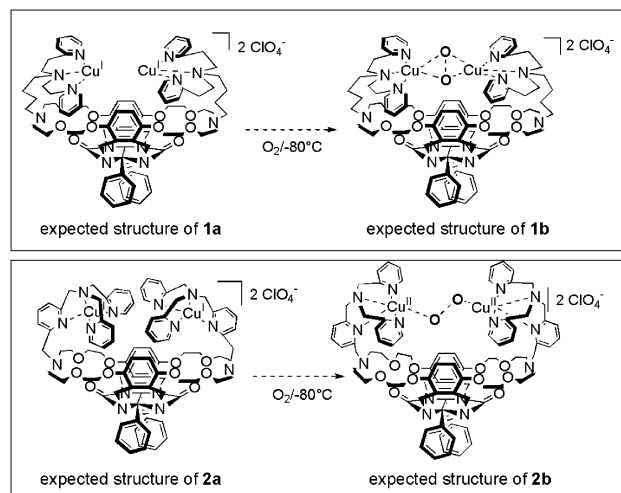


Fig. 1 Expected mode of dioxygen binding by **1a** (= **1**-Cu(I)<sub>2</sub>) and **2a** (= **2**-Cu(I)<sub>2</sub>).

appended with PY2 ligands linked by xylene spacers (**3**) and its bis-aza crown ether analogue (**4**) (Chart 1) had in earlier studies<sup>9–12</sup> been found to bind and activate oxygen, but it was observed that the benzylic position in the xylene spacer was oxidized in preference to exogenous substrates (Fig. 2). The ligands **1** and **2** are expected to be less susceptible to oxidation of their appended ligands or linkers than their predecessor **3** with its xylene linkers. In addition, the different ligand environments for the Cu(I) complexes (three-coordinated in **1a**, the bis-Cu(I)

† Based on the presentation given at Dalton Discussion No. 8, 7–9th September 2005, University of Nottingham, UK.

‡ Electronic supplementary information (ESI) available: Experimental describing the preparation of the complexes, and the catalytic, UV, and XAS experiments. Figures for the best simulations of the EXAFS, including one highlighting the Cu contribution, and complete Tables with the EXAFS simulation parameters and electrospray MS data for the Fe complex of **2**. See <http://dx.doi.org/10.1039/b506288h>

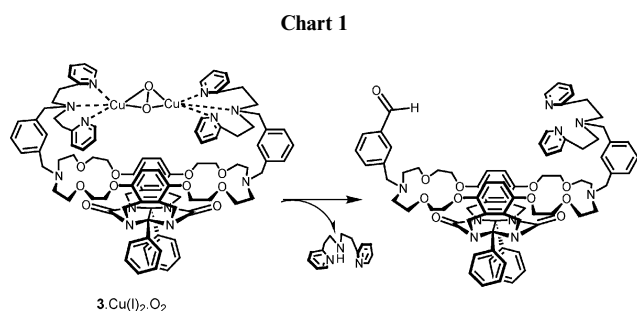
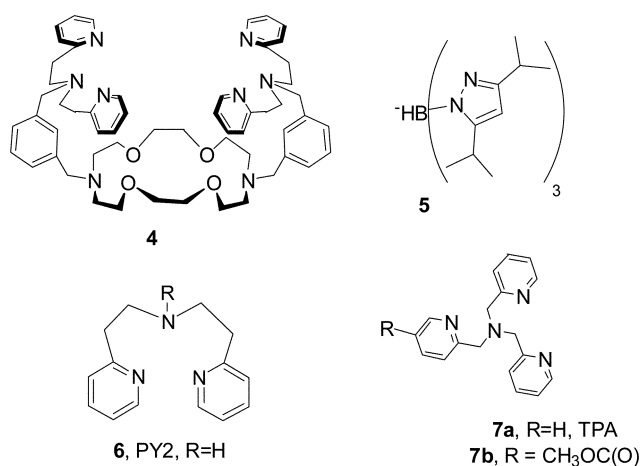
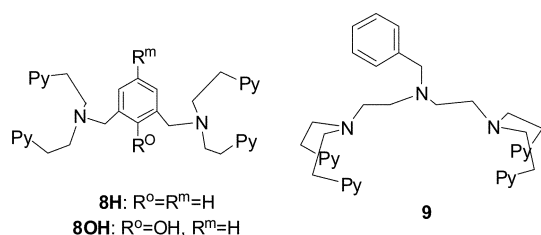


Fig. 2 Degradation of the oxygenated bis-Cu(I) complex of **3** by oxidative *N*-dealkylation.

complex of the PY2-appended ligand **1**, and four-coordinated in **2a**, the bis Cu(I) complex of the TPA-appended ligand **2**, can be expected to lead to Cu<sub>2</sub>O<sub>2</sub> complexes with different geometries (Fig. 1).<sup>13–15</sup> The  $\mu$ - $\eta^2$ : $\eta^2$  geometry for a Cu<sub>2</sub>O<sub>2</sub> unit was established by crystallography for  $\{(\mathbf{5}\cdot\text{Cu}(\text{I}))_2\cdot\text{O}_2\}$ <sup>16,17</sup> and hemocyanin<sup>1</sup> and by spectroscopy for non-substituted PY2 (**6**),<sup>14</sup> whereas the *trans*- $\mu$ -1,2 peroxo geometry was found in the crystal structure for non-substituted TPA (**7a**).<sup>18</sup>

Although the reactivity of synthetic copper dioxygen complexes is difficult to tune, the different geometries of the Cu<sub>2</sub>O<sub>2</sub> units can also be expected to result in different reactivities.<sup>14</sup> An increasing number of copper dioxygen complexes are reported to undergo ligand oxidation, either by accident or by design, as in the example of the *m*-xylyl-basket **3**<sup>10,11</sup> discussed above. The first active mimic of dinuclear copper enzyme was the bis-Cu(I) complex of the ligand with two *m*-xylyl-linked PY2 units (**8H**) (Chart 2), which gave a  $\mu$ - $\eta^2$ : $\eta^2$  complex upon binding of dioxygen and displayed hydroxylation of the *m*-xylyl spacer to give **8OH**.<sup>19</sup> More recently, ligand oxidation (either *N*-oxo transfer or *N*-dealkylation) was reported for a similar complex.<sup>20</sup> Examples of oxidation of exogenous substrates that have been reported in the literature include hydrogen atom abstraction from dihydroanthracene (>80% anthracene) and 1,4-cyclohexadiene (>70% benzene) by a mixed  $\mu$ - $\eta^2$ : $\eta^2$ /bis- $\mu$ -oxo copper dioxygen complex,<sup>21</sup> aromatic hydroxylation of lithium phenolates to the corresponding catechols by a  $\mu$ - $\eta^2$ : $\eta^2$  copper dioxygen complex,<sup>22</sup> radical coupling of phenolic substrates at the *ortho*- and *para*-positions,<sup>21</sup> and catechol



oxidation of 2,3-di-*tert*-butylcatechol by a benzimidazole-based  $\mu$ - $\eta^2$ : $\eta^2$  copper peroxo complex.<sup>23</sup>

The preparation of the ligands **1** and **2** and the respective bis-Cu(I) complexes **1a** and **2a** will be described elsewhere.<sup>8</sup> Herein, we present a study by UV-vis and X-ray absorption spectroscopy of the oxygenation of **1a** and **2a**, using our specially developed low-temperature cell.<sup>24</sup> Furthermore, the catalytic activities of **1a** and **2a** as well as some other metal complexes (Fe, Mn) of **1** and **2** in a number of oxidation reactions are explored.

## Results and discussion

### 1. UV-Vis studies of the oxygenation

**1a.** Oxygenation of deoxy species **1a** to oxy species **1b** was studied using acetone as a solvent at a temperature of  $-80$  °C (Fig. 3(A)). The absorption spectrum of **1a** showed a small band at 340 nm ( $\epsilon$  6500 M<sup>-1</sup> cm<sup>-1</sup>) that is assigned to pyridine-to-Cu metal-to-ligand charge-transfer (MLCT) (Fig. 3(A), solid line). The extinction coefficient  $\epsilon$  of the 340 nm band per Cu ion (3250 M<sup>-1</sup> cm<sup>-1</sup>) is comparable to that found for PY2-dendrimers<sup>25</sup> and PY2-appended receptors,<sup>26</sup> which amount to 3250 and 2500 M<sup>-1</sup> cm<sup>-1</sup>, respectively. Furthermore, no d-d transition band was visible in the absorption spectrum of **1a**, indicating the presence of a d<sup>10</sup> Cu(I)-species.

The colour of the solution of **1a** in acetone changed from light yellow to dark yellow/light brown upon oxygenation, and the Cu(I) band decreased (340 nm) in intensity, while two other bands were formed. The final spectrum of **1b** (Fig. 3(A), dashed line) showed features at 364 nm ( $\epsilon$  15150 M<sup>-1</sup> cm<sup>-1</sup>), which is similar to those described in the literature for other oxygenated model complexes,<sup>13</sup> and at 530 nm ( $\epsilon$  360 M<sup>-1</sup> cm<sup>-1</sup>), which is attributed to oxidation to a Cu(II) complex. As noted before for model complexes,<sup>13</sup> the  $\epsilon$  values are relatively low compared to those of oxyhemocyanin ( $\epsilon$  21000 (350 nm), 1000 (570 nm) and 200 M<sup>-1</sup> cm<sup>-1</sup> (700 nm)). The disappearance of the absorption band at 340 nm indicates that oxidation of Cu(I) to Cu(II) occurs, in line with the proposal that each Cu(I) donates one electron to the dioxygen ligand. The strong absorption at 364 nm arises from oxygen  $\pi_{\sigma}^*$  to Cu(II) charge transfer<sup>15</sup> and the position of this band is characteristic for a side-on binding of dioxygen. We conclude that **1b** shows the expected dioxygen binding mode, namely a Cu(II)<sub>2</sub>(O<sub>2</sub><sup>2-</sup>) complex with  $\mu$ - $\eta^2$ : $\eta^2$  geometry (Fig. 1, top).

The oxygenation of **1a** to **1b** was also investigated in dichloromethane (Fig. 3(B)), a solvent in which diphenylglycoluril clips and baskets display the receptor properties required for supramolecular catalysis, and in THF (with acetonitrile, Fig. 3(C)). The geometry of the Cu<sub>2</sub>O<sub>2</sub> complex (bis- $\mu$ -oxo vs.  $\mu$ - $\eta^2$ : $\eta^2$ ) formed by oxygenation of some Cu(I) complexes such as those with ligand **9**<sup>27–31</sup> has been found to vary in these solvents, and the bending of the  $\mu$ - $\eta^2$ : $\eta^2$  Cu<sub>2</sub>O<sub>2</sub> unit in oxygenated **3**-Cu(I)<sub>2</sub> increased upon going from acetone to THF.<sup>12</sup> The spectrum of **1b** in dichloromethane (Fig. 3(B), dashed line) was comparable to that in acetone, with somewhat lower values for  $\epsilon$ , *viz.* 12600 (364 nm) and 210 M<sup>-1</sup> cm<sup>-1</sup> (530 nm). No oxygenation band was observed for THF (Fig. 3(C), dashed line), probably because of the necessity to use acetonitrile as a co-solvent (final composition: THF–acetonitrile 70/30), which may interfere with the oxygenation by coordinating to Cu(I) itself.

The formation of **1b** from **1a** in acetone was monitored in time by measuring the UV-vis absorption at 364 nm and found to be exponential in time, and complete within 10 min; **1b** was found to be stable at  $-80$  °C for at least 90 min (Fig. 3(D)). Dioxygen binding in **1b** was irreversible, as the application of vacuum and argon purges (arrow in Fig. 3(D)) had no effect. When the solution of **1b** was allowed to warm up from  $-80$  °C till room temperature, however, the absorption at 364 nm collapsed rapidly. When the resulting solution was evaporated to dryness,

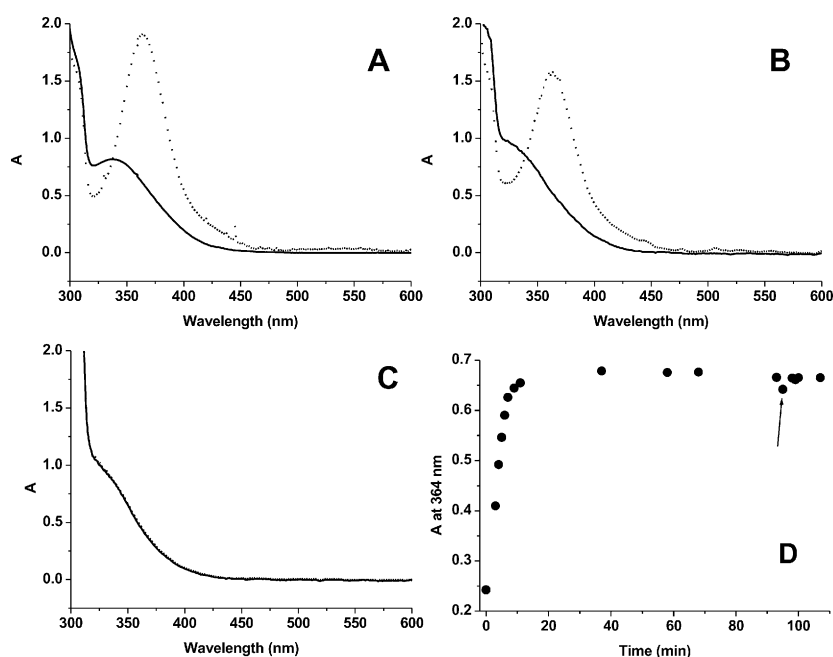


**Fig. 3** Absorption spectra of **1a** (solid) and **1b** (dashed) at  $-80\text{ }^{\circ}\text{C}$ : top left (A), acetone; top right (B), dichloromethane; bottom left (C), THF-acetonitrile (70/30, v/v). Bottom right (D): Absorption at  $\lambda_{\text{max}}$  (364 nm) of **1b** in acetone at  $-80\text{ }^{\circ}\text{C}$  in time, argon/vacuum purges (see text) at arrow. The base lines of the spectra were adjusted by subtracting the values of the absorption at 650 from the measured spectra.

redissolved in chloroform, and extracted with aqueous  $\text{NH}_3$  to remove the Cu ions, receptor **1** was recovered unchanged as observed by  $^1\text{H}$  NMR. This is an interesting difference in behaviour when compared to the oxygenated bis-Cu(I) complex of **3**, the xylyl analogue of **1**, which was found to undergo oxidative *N*-dealkylation at the benzylic position, even at  $-80\text{ }^{\circ}\text{C}$  (Fig. 2).<sup>11</sup> The apparent stability of **1b** at low temperature allowed us to investigate the stoichiometry of the dioxygen binding by a low temperature UV-vis titration, rather than by manometry,<sup>11,32</sup> which would have required much more material. This titration was carried out by adding precisely defined amounts of dioxygen, as a 1.00% mixture in argon, to a solution of **1a** in acetone at  $-80\text{ }^{\circ}\text{C}$ , in aliquots corresponding to exactly 0.5 molar equivalents with respect to the dinuclear copper complex, to a maximum of 1.5 equivalents. The time needed for complete oxygenation was 4 h, which is much slower than with excess dioxygen (10 min). The absorption at 364 nm increased till 1.0 equivalent had been added, after which it stayed at the same level. This result confirms that one molecule of oxygen per dinuclear copper unit is bound, in line with the formation of a  $\mu\text{-}\eta^2\text{:}\eta^2\text{ Cu}_2\text{O}_2$  moiety as proposed above.

In order to determine whether the oxygen binding is intermolecular or intramolecular, *i.e.* involving Cu(I) ions bound to PY2 units of the same or of different ligand molecules of **1**, respectively, the rate of oxygen binding was estimated as a

function of the concentration of **1a** between 0.25 and  $1.0 \times 10^{-4}\text{ M}$ . As the rate increased proportionally with concentration, it was concluded that the oxygen is bound intramolecularly. The rate of oxygenation was also first order in oxygen, as estimated from experiments where the addition of oxygen was controlled by the bubbling frequency.

**2a.** UV-Vis spectroscopy on the deoxy and oxy forms of the Cu complexes of receptor **2** was carried out at low temperature ( $-80\text{ }^{\circ}\text{C}$ ) in dichloromethane and the results are depicted in the left panel of Fig. 4. The UV-vis spectrum of Cu(I) complex **2a** (solid line) showed a band at 360 nm ( $\epsilon$  18000  $\text{M}^{-1}\text{ cm}^{-1}$  or 9000 per copper ion), assigned to the pyridine nitrogen to copper MLCT band. No d-d transition band was found, indicating the presence of a  $d^{10}$  species, which confirms that copper is present as copper(I). This is similar to what was observed for receptor **1** described above. No significant changes were observed in the spectrum after warm-up at room temperature (not shown). The expected mode of dioxygen binding for a receptor comprising TPA units is dinuclear  $\text{Cu}_2\text{O}_2$  end-on peroxy (Fig. 1, bottom), with characteristic absorption bands at 525 nm ( $\epsilon$  11500  $\text{M}^{-1}\text{ cm}^{-1}$ ) and 590 nm ( $\epsilon$  7600  $\text{M}^{-1}\text{ cm}^{-1}$ ).<sup>33,34</sup> When the uptake of dioxygen by **2a** was studied in time at  $-80\text{ }^{\circ}\text{C}$  (Fig. 4, right) none of the above-mentioned characteristic absorption bands appeared; it must therefore be concluded that there is no

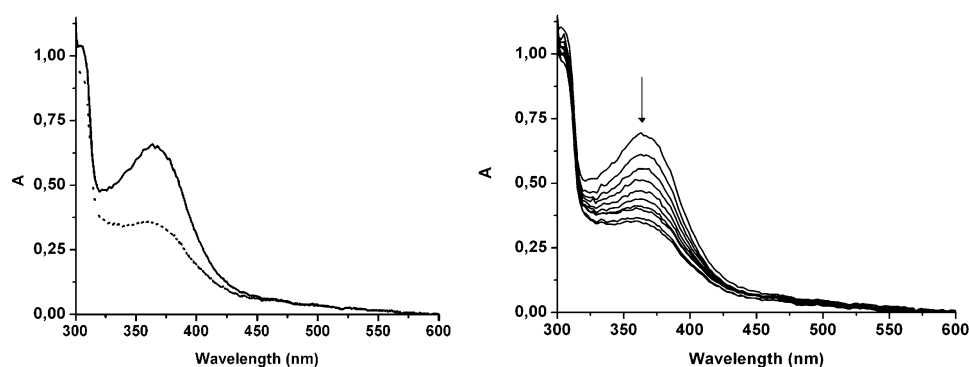


**Fig. 4** Absorption spectra in dichloromethane at  $-80\text{ }^{\circ}\text{C}$ . Left, absorption spectra of **2a** (solid) and **2b** (dashed); right,  $\text{O}_2$  uptake in time (1 scan/2 min) with arrow indicating the decrease of the absorption at 340 nm in time. The base lines of the spectra were adjusted by subtracting the values of the absorption at 650 nm from the spectra.

formation of an end-on peroxide copper–dioxygen complex. A decrease in the band at 340 nm is however observed, indicating oxidation of Cu(I) to Cu(II) or Cu(III). When the solution was allowed to warm up to room temperature, the band at 340 nm disappeared completely. In separate experiments, the rate of oxidation at  $-80\text{ }^{\circ}\text{C}$  was found to be proportional to the bubbling frequency by which the oxygen addition was controlled.

It is somewhat surprising that the expected  $\text{Cu}_2\text{-(O}_2\text{) trans-}\mu\text{-1,2-peroxo dicopper(II)}$  complex does not form. The most likely explanation is that the attachment to the diphenylglycoluril basket platform does not allow the TPA–Cu(I) moieties to assume the required orientation with respect to each other; alternatively, the solvent dichloromethane could have interfered, but the chloro-copper(II) complexes resulting from such an interference were not detected in our EXAFS study (see below).<sup>35,36</sup>

## 2. X-Ray absorption spectroscopic studies of the oxygenation

**Effect of oxygenation on the X-ray absorption near-edge structure (XANES).** The XANES of **1a** (Fig. 5, solid trace A) has an edge energy of approximately 8985 eV, which is characteristic of a Cu(I) model compounds,<sup>37</sup> and comparable to deoxy hemocyanin;<sup>38</sup> it can thus be concluded that the copper in **1a** is present as Cu(I), as expected. The XANES of **1a** also shows a pre-edge transition, due to excitation of the 1s electron to unoccupied higher orbitals; the position and transition probability of this pre-edge transition are determined by the symmetry of the ligand environment, and hence by the coordination number.<sup>37,38</sup> The pre-edge transition of **1a** was found to be surprisingly weak in comparison to that of the Cu(I) complex of **4**, studied previously by our group.<sup>12</sup> This weakness is possibly due to deviations from a symmetric tri-coordinate Cu(I) complex; it is however not clear from the XANES what the exact nature of these deviations is.

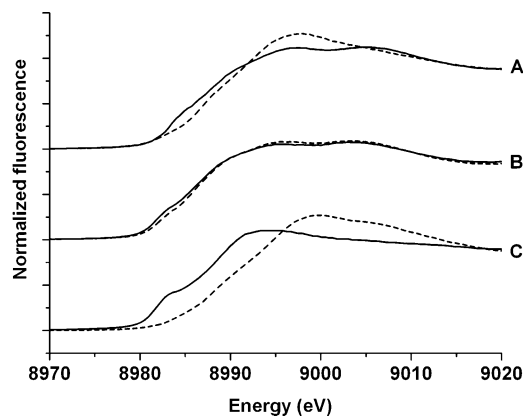


**Fig. 5** Effect of oxygenation on the XANES spectra of **1a** and **1b**. Trace A, **1a** (solid) and **1b** (dashed) in acetone; trace B, **1a** (solid) and **1b** (dashed) in THF–acetonitrile (70/30); trace C, **2a** (solid) and **2b** (dashed) in acetone.

Considerable changes were observed in the XANES spectrum upon oxygenation of **1a** in acetone, to give **1b** (Fig. 5, dashed trace A), *viz.* a shift in the edge position as well as a change in the shape to a smoother curve without a pre-edge transition; these results indicate the formation of a Cu(II) complex. The results obtained for **1b** in frozen acetone are very similar to the data obtained for oxy hemocyanin<sup>38</sup> as well as the oxy complex of **4**.<sup>12</sup> It is worth noting that attempts to characterize oxygenated Cu(I) complexes of **3**, the xylyl analogue of **1**, by XAS failed because the samples were found to be too dilute, too incompletely oxygenated, or to be decomposed.<sup>12</sup> The present success in characterizing the oxygenated **1b** was possible only due to the application of our specially developed dual setup for the UV-vis and XAS measurements,<sup>24</sup> which allows low-temperature UV-vis characterization of XAS samples prior to XAS data

collection. This new experimental approach was explored in some more detail. A fully oxygenated sample, as judged by the XANES, could be obtained by bubbling dioxygen through a solution of **1a** at  $-80\text{ }^{\circ}\text{C}$  at a concentration of 1 mM, but this was too concentrated to determine the UV-vis absorption. For more dilute solutions, longer exposure to oxygen was needed, but as care had to be taken not to heat the sample too much, this time was limited to 10 min. For example, a sample with a concentration of **1a** of  $1.0 \times 10^{-4}\text{ M}$  showed an apparent extinction coefficient at 364 nm of  $12300\text{ M}^{-1}\text{ cm}^{-1}$ , corresponding to 81% oxygenation; when the XANES of this very sample was simulated with varying contributions of deoxygenated and oxygenated spectra, following a procedure reported before to establish the degree of oxygenation of hemocyanin crystals,<sup>38</sup> exactly the same degree of oxygenation as derived from the UV-vis was found. For a sample of **1b** prepared in the same way as previously attempted for oxygenated **3**,<sup>12</sup> the XANES (not shown) not only deviated from either pure **1a** or **1b**, but also from any linear combination thereof, presumably because other oxidized dinuclear Cu species with different XANES features, such as  $\text{Cu(II)}_2(\text{OH})_2$ , had been formed; the extent of oxygenation (or oxidation) was therefore more difficult to determine accurately, but is estimated at between 40 and 70%.

The XANES spectrum of **1a** in THF–acetonitrile (70/30) (Fig. 5, solid trace B) is characteristic for Cu(I), but has a slightly lower energy (1 eV) than **1a** in acetone. The pre-edge transition was weaker than that of **1a** in acetone (see above). This indicates that the Cu(I) environment in **1a** in THF–acetonitrile has an even lower symmetry than in acetone, and is consistent with the formation of a tetra-coordinate complex, possibly due to the coordination of a solvent molecule of acetonitrile to Cu(I). No significant edge shift was observed upon oxygenation of **1a** in THF–acetonitrile (Fig. 5, dashed trace B); the only detectable effect was the disappearance of the pre-edge feature. This result indicates that only partial oxidation of Cu(I) to Cu(II) has occurred. This low extent of oxidation upon addition of dioxygen has been reported previously for **4** in pure acetonitrile,<sup>12</sup> and has been ascribed to strong coordination of acetonitrile to the Cu(I) complex, inhibiting dioxygen binding. Our results suggest that 30 vol% of acetonitrile is enough to efficiently block the binding of dioxygen. The XANES result is in line with absence of any effect of oxygenation on the UV-vis spectrum.

The position of the edge for **2a** (Fig. 5, solid trace C) confirmed the valence of Cu(I) for this complex. The relatively prominent presence of the pre-edge transition observed for **2a** could point to tri-coordination to the copper ion.<sup>37</sup> However, more than three possible donor atoms are present in the vicinity of the copper ion in complex **2a**, *viz.* three pyridyl nitrogen donors and one amino nitrogen donor, which in principle allows for tetra-coordination. In the literature, however, there are other examples of tri-coordination by TPA ligands, both in solution<sup>39</sup> and the solid state.<sup>40</sup>

In earlier studies,<sup>12</sup> dichloromethane was found to be not a suitable solvent for XAS studies because of the scattering by the relatively large chlorine atoms; therefore, no attempts were made to study **1** and **2** by XAS in this solvent.

**EXAFS of the Cu(I) complexes.** As can be seen in Fig. 6, subtle differences can be observed both in the EXAFS and Fourier transform between the deoxy spectra of the three samples (solid lines), *viz.* **1a** in acetone (traces A), **1a** in THF–acetonitrile (B), and **2a** in acetone (C). Upon oxygenation of these deoxy species in acetone (**1a** to **1b**, and **2a** to **2b**) prominent changes were observed; an increase in the amplitude of the  $k^3$ -weighted EXAFS was visible for both **1b** and **2b**, when compared to **1a** and **2a**, as well as an approximate doubling of the intensity of the Fourier transform of the main shell of low-Z atoms at 2 Å. However, for oxygenation of **1a** in THF–acetonitrile the change was much less pronounced. Detailed simulations of the Fourier-filtered EXAFS and Fourier-filtered Fourier transforms

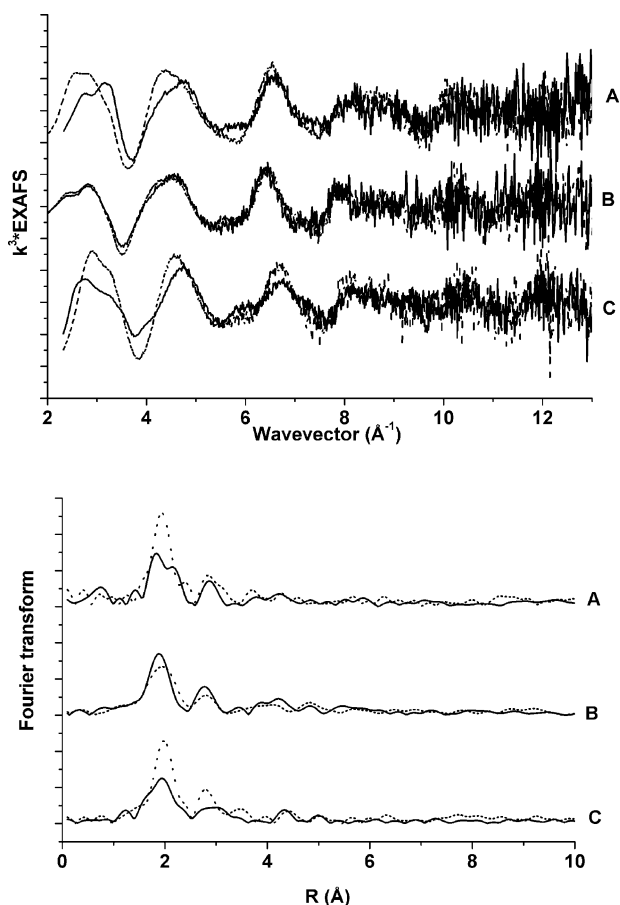
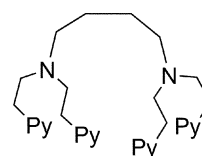


**Fig. 6**  $k^3$ -Weighted EXAFS (top panel) and corresponding phase-corrected Fourier transforms (bottom panel) of bis-Cu(I) complexes in the absence (solid traces) and presence (dashed traces) of oxygen, of **1** in acetone (traces A), **1** in THF-acetonitrile (70/30) (traces B), and of **2** in acetone (traces C).

were carried out using the programme EXCURV98, following an approach adapted from earlier EXAFS analyses<sup>12</sup> (see also ESI†). The analysis started with iterative refinements of single scattering simulations of the Fourier-filtered major shells (around 1.5–2.0 Å) using nitrogen atoms in order to discern trends in coordination numbers, as presented in Table 1. The results showed an increase in coordination number upon going from acetone to THF-acetonitrile, from a typical value of three nitrogen atoms in acetone to four nitrogen atoms in THF-acetonitrile. Furthermore, a difference in average ligand distance (Cu–N) was observed between the complexes of receptors **1**, **1a** and **1b** (1.96–1.98 Å), and the complexes of receptors **2**, **2a** (2.015 Å) and **2b** (1.996 Å).

In the refined simulation of long-range Fourier-filtered EXAFS for deoxy complex **1a** in acetone (parameters in Table 2, entry 1), it was found that two pyridyl nitrogen donors and one aliphatic amino nitrogen donor at 1.954 and 2.098 Å, respectively, are involved in the coordination. This result was expected on the basis of earlier EXAFS experiments of PY2 systems,<sup>41,12</sup> and the known crystal structures of Cu(I) complexes with PY2 ligands. For example, the crystal structure of [Cu<sub>2</sub>(**10**)](ClO<sub>4</sub>)<sub>2</sub><sup>42</sup> (**10** = N4PY2, Chart 3) contains tetra-coordinate copper, which has an environment of two pyridyl groups (average 1.939 Å) and one amine nitrogen donor (2.145 Å) as well as an oxygen donor of the perchlorate counter ion (2.547 Å), but can be considered tri-coordinate in view of the weak coordination of the perchlorate anion.



**10**, N4PY2

**Chart 3**

**Table 1** Analysis of main Fourier-filtered shells of Cu complexes with single scattering theory. The refined parameters were the threshold energy,  $\Delta E$ , the occupancy, the Cu–N distance  $R$ , and the Cu–N Debye–Waller-type factor, expressed as  $2\sigma^2$

Entry	Complex	Cell type	Range/Å	Energy range/eV	$\Delta E$ /eV	No. Cu–N	$R$ /Å	$2\sigma^2/\text{Å}^2$
1	<b>1a</b> <sup>a,c</sup>	Old	0.6–2.4	18–500	–0.354	3.0	1.960	0.021
2	<b>1b</b> <sup>a,c</sup>	New	0.8–2.4	18–600	–3.748	3.3	1.996	0.010
3	<b>1b</b> <sup>a,d</sup>	New	0.9–2.2	18–550	–0.461	3.2	1.978	0.022
4	<b>1a</b> <sup>b,c</sup>	Old	0.8–2.4	18–675	–3.049	3.9	1.963	0.011
5	<b>1b</b> <sup>b,c</sup>	Old	0.9–2.5	18–675	–3.136	3.8	1.977	0.012
6	<b>2a</b> <sup>a,d</sup>	Old	0.8–2.4	18–500	–3.947	3.1	2.015	0.016
7	<b>2b</b> <sup>a,c</sup>	Old	0.8–2.4	18–600	–1.966	3.2	1.996	0.015

Solvent:<sup>a</sup> acetone; <sup>b</sup> a mixture of THF and acetonitrile (7:3); Conc.:<sup>c</sup> 1–2 × 10<sup>−3</sup> M; <sup>d</sup> 1 × 10<sup>−4</sup> M.

**Table 2** Parameters for refined multiple scattering simulations of the bis-Cu(I) complexes **1a** and **2a**<sup>a,b</sup>

Entry	1	2	3
Sample	<b>1a</b> in acetone	<b>1a</b> in THF-ACN	<b>2a</b> in acetone
	A <sup>c</sup>	B <sup>c</sup>	C <sup>c</sup>
Range/eV	3.0–550.0	3.0–575.0	3.0–675.0
$\Delta E$ /eV	–2.2338	–5.126	–3.763
Pyr-N <sup>d</sup>	2.1 @ 1.954 (0.009)	2.1 @ 1.984 (0.010)	1.0 @ 1.958 (0.007)
Amine-N	0.9 @ 2.098 (0.001)	0.8 @ 2.103 (0.003)	1.1 @ 2.048 (0.009)
Cu–Cu	No sign. contribution	No sign. contribution	No sign. contribution
Fit index <sup>e</sup>	0.1624	0.2011	0.3859

<sup>a</sup> Distances in Å; Debye–Waller-type factors as  $2\sigma^2$  in parentheses in Å<sup>2</sup>. <sup>b</sup> Errors in main shell distances 0.03 Å, other shells 0.05 Å. <sup>c</sup> See Fig. S1 in ESI.† <sup>d</sup> For other pyridine ring parameters, see Table S1 in ESI.† <sup>e</sup> Fit index on FF-data  $k^3$ -weighting.

**Table 3** Parameters for simulations of the Cu(II) complexes of **1b** and **2b**<sup>a,b</sup>

Entry	1	2	3	4
Complex	<b>1b</b> in acetone, conc.	<b>1b</b> in acetone, dil.	<b>1b</b> in THF–ACN	<b>2b</b> in acetone
	A <sup>c,d</sup>	B <sup>c</sup>	C <sup>c</sup>	D <sup>c</sup>
Range/eV	3.0–460.0	3.0–460.0	3.0–675.0	3.0–675.0
$\Delta E$ /eV	–5.844	–4.605	–3.026	–6.910
Pyr-N <sup>e</sup>	2.5 @ 2.027 (0.018)	1.7 @ 2.030 (0.012)	2.3 @ 2.014 (0.013)	1.3 @ 2.066 (0.002)
Amine-N	No sign. contribution	No sign. contribution	No sign. contribution	0.6 @ 2.241 (0.001)
O <sup>g</sup>	0.8 @ 1.887/1.964 (0.002) <sup>c</sup>	0.9 @ 1.866/1.984 (0.001)	0.8 @ 1.947 (0.012)	2.0 @ 1.952 (0.011)
Cu <sup>g</sup>	0.8 @ 3.593 (0.020)	0.9 @ 3.486 (0.022)	No sign. contribution	1.7 @ 2.909 (0.030)
Fit index <sup>f</sup>	0.0767	0.0886	0.1369	0.0749

<sup>a</sup> Distances in Å; Debye–Waller-type factors as  $2\sigma^2$  in parentheses in Å<sup>2</sup>. <sup>b</sup> Errors in main shell distances 0.03 Å, other shells 0.05 Å; <sup>c</sup> See Fig. S2 in ESI.† <sup>d</sup> See Fig. S3 in ESI† for highlighted Cu contribution. <sup>e</sup> For other pyridine ring parameters, see Table S2 in ESI.† <sup>f</sup> Fit index on FF-data  $k^3$ -weighting. <sup>g</sup> The Cu<sub>2</sub>O<sub>2</sub> moiety has been refined as a unit with all occupancies refined at the same value.

The results of the simulation for deoxy complex **1a** in THF–acetonitrile (Table 2, entry 2) suggest two coordinating pyridyl groups (average 1.984 Å) and one amino nitrogen donor (2.103 Å). The Cu–N(pyridine) distance has increased significantly from 1.954 to 1.984 Å, going from acetone to THF–acetonitrile. This trend for longer Cu–N(pyridine) distances is in line with the crystallographic data of [Cu<sub>2</sub>(**10**)(CH<sub>3</sub>CN)<sub>2</sub>](ClO<sub>4</sub>)<sub>2</sub><sup>43</sup> which has pseudo-tetrahedral geometry, and an average Cu–N(pyridine) distance of 2.024 Å and Cu–N(amine) and Cu–N(acetonitrile) distances of 2.151 and 1.945 Å, respectively. The change in distances going from **1a** in acetone to **1a** in THF–acetonitrile clearly points to some effect of acetonitrile, indicating solvent coordination. This is also reflected in the single shell analysis which gives an occupancy of almost four (see above). An attempt to analyse the data by multiple shell simulations including also contributions of acetonitrile had to be abandoned because of heavy correlations between the shells. Nevertheless, there is considerable indirect evidence, *viz.* from the significant longer Cu–N(pyridine) distance as well as the increased occupancy in the single-shell simulation and the change in edge profile (see above), for the coordination of an acetonitrile molecule to copper. This is in line with our proposal (see above) that acetonitrile can interfere with the oxygenation by binding to Cu(I).

The single shell analysis of the EXAFS **2a** in acetone (Table 1) revealed that there are no more than three nitrogen donor ligands, implying that not all pyridyl groups and amino nitrogen donors are coordinated to Cu(I). In line with this result, the detailed analysis (Table 2, entry 3) indeed showed that not all pyridyl moieties were coordinated to copper. There is also evidence from crystallographic studies that the TPA ligand can coordinate with varying numbers of pyridine ligands. One example of a copper complex with three coordinating pyridyl groups is the Cu(I) complex of 5-carbomethoxy-TPA (**7b**), having a pseudo tetra-coordination with the following geometry: Cu–N(acetonitrile) 1.999 Å; Cu–N(pyridine) 2.093, 2.130, 2.108 Å and Cu–N(amine) 2.439 Å.<sup>41</sup> In the presence of a stronger ligand, such as PPh<sub>3</sub>, one of the pyridyl groups of TPA can be displaced; this is described in the literature<sup>41</sup> for [7-Cu(PPh<sub>3</sub>)](PF<sub>6</sub>) having a tetra-coordinate Cu(I) ion: Cu–N(amine) 2.248 Å, Cu–N(pyr) 2.047 and 2.094 Å and Cu–P 2.194 Å, with one “free dangling” pyridyl group.

For complex **2a** in acetone, the simulation indicated that one or at most two pyridine ligands rather than three are coordinated to each Cu(I) ion at 1.958 Å, in addition to 1–2 amino nitrogen donors at 2.048 Å. When the occupancies were varied in half-integer steps, the best simulation was obtained with an occupancy of 1.5 for both Cu–N(amine) and Cu–N(pyridine). This is in line with our NMR results,<sup>8</sup> which showed possible inclusion of pyridine rings in the cavity of the diphenylglycoluril host, and a role for amine nitrogen donors, including the aza

crown ether N-donors, in the Cu coordination. NMR studies have indicated that the coordination of a TPA ligand to copper is dynamic and that at no time all of the pyridyl moieties are coordinated to copper.<sup>39,43</sup>

**EXAFS of the oxygenated complexes.** The XANES measurements with the dual UV-vis/EXAFS set-up<sup>24</sup> using a dilute sample gave 81% oxygenation, with the remaining part being Cu(I). In spite of this, the experimental and simulated curves of the EXAFS and Fourier transforms of spectra A and B (parameters in Table 3, entries 1 and 2) corresponding to the concentrated and dilute samples, respectively, do not show large differences. The optimum fit for the copper contribution in sample B was found at a Cu–Cu distance of 3.593 Å with an almost fully extended (flat)  $\mu$ - $\eta^2$ : $\eta^2$  Cu<sub>2</sub>O<sub>2</sub> moiety, in agreement with the copper–dioxygen complex found in hemocyanin<sup>1</sup> and Kitajima’s model complex.<sup>16,17</sup> A dihedral angle of 140° had been observed for the copper complex of **4**, based on a Cu–Cu distance of 3.31 Å from the EXAFS data,<sup>12</sup> giving it a butterfly structure. The elongation of the metal–metal distance must be induced by the change in both the crown ether scaffold (basket *vs.* diaza crown ether) and spacer (butyl *vs.* *m*-xylylene).

In line with what was observed for the XANES (Fig. 5(B)), only small changes were found (Fig. 6(B)) for either the EXAFS or the Fourier transform upon oxygenation of **1a** to **1b** in THF–acetonitrile (70/30). As discussed above for the XANES and EXAFS of **1a**, there is considerable indirect evidence (lengthening of the Cu–pyridine distances derived from the EXAFS, increased occupancy of the first shell and change in edge profile) that acetonitrile coordinates to Cu(I) in this complex, and this is likely to interfere with oxygenation. The refined simulation (Table 3, entry 3) did, however, show an occupancy of 0.8 for an oxygen atom (at 1.947 Å) in **1b** and a difference in the C–N(pyridine) distance, going from 1.984 for **1a** to 2.014 Å for **1b**, respectively. One might consider Cu(II)<sub>2</sub>(OH)<sub>2</sub> as a possible structure for the metal site in **1b** in THF–acetonitrile. In the literature the following distances are reported for a Cu(II)<sub>2</sub>(OH)<sub>2</sub> complex of a bis-PY2-appended *m*-xylene **8**: a Cu–O(hydroxyl) distance of 1.938/1.962 (*cf.* 1.947 for **1b**), a relatively long Cu–N(pyridine) distance of 2.006/2.027 (*cf.* 2.014 for **1b**);<sup>19</sup> on the other hand, the crystal structure also features a Cu–N(amine) distance of 2.034/2.028 and a Cu–Cu distance of 3.082 Å, neither of which was found in the EXAFS of **1b**. Thus, it is concluded that **1a** was partly oxidized to a new species with an additional oxygen ligand upon oxygenation in THF–acetonitrile, and that the reaction occurred to an extent that was significant enough to shift the average ligand distances to values more characteristic of Cu(II). It must be emphasized, however, that the changes in THF–acetonitrile are very small compared to the effect of oxygenation of **1a** in acetone.

The XANES (Fig. 5(C)) had revealed that oxidation from Cu(I) to Cu(II) occurs upon addition of dioxygen to a solution of **2a** in acetone, consistent with the disappearance of the 340 nm band in the UV-vis spectrum. However, no distinct copper-dioxygen bands were observed in the UV-vis spectrum of **2b** in dichloromethane (Fig. 4) either at 364 nm (indicative of a  $\mu\text{-}\eta^2\text{-}\eta^2$  complex) or at 550 nm (indicative of a *trans*  $\mu\text{-}1,2$  complex). The result of the single scattering simulations for the EXAFS of **2b** (Table 1) showed a slight increase in coordination upon oxygenation. The intensity of the Fourier transform in the main shell at 2 Å showed a significant increase and refined simulations revealed that there are at most two of the three possible pyridines, more possibly only one per copper ion (at 2.066 Å), along with one N-donor with a Cu–N(amine) of 2.241 Å, two oxygens at 1.952 Å, and a very close Cu at 2.909 Å.

This result is not wholly consistent with either the geometry derived from the crystallographically characterized *trans*  $\mu\text{-}1,2$  peroxo Cu(II)<sub>2</sub>O<sub>2</sub> complex of TPA **7a**,<sup>18</sup> which has a Cu–Cu distance of 4.349 Å (*cf.* 2.909 for **2b**), Cu–N(pyridine) distances of 2.024/2.104/2.102 Å (*cf.* 2.066 for **2b**), and Cu–N(amine) of 2.104 Å (*cf.* 2.241 for **2b**) or with that of the crystallographically characterized Cu(II)<sub>2</sub>(OH)<sub>2</sub> complex of **8** mentioned above<sup>19</sup> which has relatively short Cu–O(hydroxyl) distances of 1.938/1.962 Å (*cf.* 1.952 for **2b**), relatively long Cu–N(pyridine) distances of 2.006/2.027 Å (*cf.* 2.066 for **2b**), relatively short Cu–N(amine) distances of 2.034/2.028 Å (*cf.* 2.241 for **2b**) and a Cu–Cu distance of 3.082 (*cf.* 2.909 for **2b**). The results from the above EXAFS data and the UV-vis spectra indicate that only one or two of the three pyridyl groups of the TPA unit are coordinated to copper in **2b**, but they do not allow the structure to be defined in more detail.

### 3. Catalytic properties

#### Catalysis with the bis-Cu(I) dioxygen complex of **1 (1b)**.

A well-known guest for diphenylglycoluril baskets such as **1** and **2** is resorcinol, for which binding constants in the range 2000–3100 M<sup>-1</sup> have been reported for a variety of basket molecules.<sup>44–46</sup> The reactivity of the copper dioxygen complex of **1 (1b)** in various types of oxidative reactions was tested on this type of substrate (Fig. 7). Benzylic hydroxylation, which is carried out in Nature by *e.g.* dopamine- $\beta$ -hydroxylase, was tested with orcinol, which should afford 3,5-dihydroxybenzyl alcohol or the corresponding aldehyde. In addition, the reactivity was tested with *p*-cresol, which should afford *p*-hydroxybenzyl alcohol or aldehyde; the latter would imply oxidation of a primary alcohol such as catalyzed by galactose oxidase. Furthermore,

aromatic hydroxylation, which is carried out in Nature by *e.g.* tyrosinase, was tested with resorcinol, which should afford 1,3,5-trihydroxybenzene (phloroglucinol). The last type of oxygenation that was studied, is epoxidation, which is not carried out by copper enzymes but by iron enzymes in Nature, *e.g.* cytochrome P450. Epoxidation was tested with both limonene and styrene. Resorcinol, orcinol, and their expected oxidation products contain multiple hydroxyl groups which makes GC analysis difficult. In order to overcome this problem silylation of the hydroxyl groups was carried out. A standard silylating agent (TMSCl and (TMS)<sub>2</sub>NH)<sup>47</sup> has been used in previous research,<sup>26</sup> and although disilylation does occur, it is not quantitative. Therefore, another silylation reagent was used, namely MSTFA (*N*-(1,1,1-trimethylsilyl)-2,2,2-trifluoroacetamide), which is more reactive.

Oxidation reactions with resorcinol were carried out at –80 °C, in view of the instability of the Cu<sub>2</sub>O<sub>2</sub> complex, using three different methods (see Experimental section and Table 4). The first method entailed the formation of the Cu<sub>2</sub>O<sub>2</sub> complex prior to addition of substrate. The second method is similar, but the excess of dioxygen was removed before addition of the substrate by repeated vacuum/argon purges. The third method comprised the addition of substrate prior to addition of dioxygen. Oxidation of resorcinol was tested with method 1 and 2 (entries 1 and 2, respectively). Both experiments, unfortunately, gave only undefined brown products, which are most likely oligomeric or polymeric products, formed by radical coupling reactions. Oxidation of orcinol using method 3 gave similar results (entry 3). Oxidation of *p*-cresol was tested using two different conditions with either five molar equivalents of substrate using method 2 (entry 4) or two equivalents of substrate using method 1 (entry 5). In both cases in addition to *p*-cresol, a small broad peak was observed on GC, which however could not be attributed to the desired product 4-hydroxybenzaldehyde. Oxidation of styrene (2 equivalents) using method 2 gave no oxidation products (entry 6). Oxidation of limonene (5 equivalents) was tested with method 1 (entry 7) and method 3 (entry 8). No formation of the desired products was observed for either experiment. When 25 equivalents of ascorbate were added as a co-reductor (entry 9) many small peaks appeared at high retention times, none of which could be identified as the expected products, such as epoxide, di-epoxide and diol.

A radical coupling mechanism was thought to play a role in the above-mentioned oxidation studies with phenolic substrates, giving rise to oligomeric or polymeric products that cannot be identified. In order to test if radical coupling indeed played a role, the test substrate 2,4-di-*tert*-butylphenol was used in the

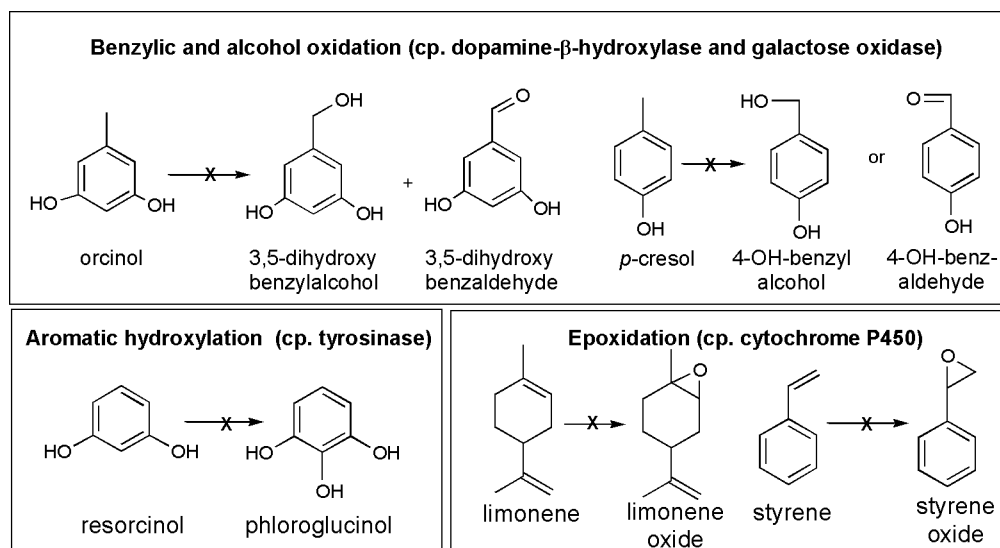


Fig. 7 Substrates in reactions with **1b** and possible oxygenation products.

**Table 4** Catalytic oxygenation experiments using the copper dioxygen complex **1b**

Entry	Substrate	Eq. of substrate	Method <sup>a</sup>	Products
1	Resorcinol	1	1	u.p. <sup>b</sup>
2	Resorcinol	3	2	u.p.
3	Orcinol	3	3	u.p.
4	<i>p</i> -Cresol	5	2	u.p.
5	<i>p</i> -Cresol	2	1	u.p.
6	Styrene	2	2	n.p. <sup>c</sup>
7	Limonene	5	1	n.p.
8	Limonene	5	3	n.p.
9	Limonene/ascorbate	5/25	1	u.p.
10	2,4-Di- <i>tert</i> -butyl phenol	5	1	1.4 TON dimer
11	2,4-Di- <i>tert</i> -butyl phenol	100	2	10 TON dimer <sup>d</sup>

<sup>a</sup> Method 1: excess of O<sub>2</sub> followed by substrate; method 2: excess of O<sub>2</sub>, removal of excess followed by substrate; method 3: substrate followed by excess of O<sub>2</sub>. More details in Experimental section. <sup>b</sup> u.p. = Unidentified products observed. <sup>c</sup> n.p. = No products observed. <sup>d</sup> After 3 h at -80 °C a TON of 1 is observed, after warming up a TON of 10 is observed.

reaction. This compound is known to give the dimeric carbon-carbon coupling product (Fig. 8),<sup>48</sup> which is easily distinguished from the starting monomer by GC analysis. Catalysis was tested with **1b** and 5 equivalents of 2,4-di-*tert*-butylphenol using method 3 (entry 10). A colour change of light yellow to green/blue was observed after addition of O<sub>2</sub>, and after warming up the yellow colour returned. GC analysis of the reaction mixture revealed C-C coupling of 28% accounting for a TON of 1.4 after warming up. When 100 equivalents of substrate were added a TON of 1 for C-C dimerisation was measured after 3 h, while a TON of 10 for the C-C dimer was found after warming up of the reaction mixture to room temperature under a dioxygen atmosphere (entry 11). At low temperature the reaction is limited by the lack of dioxygen (excess of dioxygen was removed before addition of the substrate, *cf.* method 2) resulting in the relatively low TON of 1. Thus it can be concluded that radical coupling indeed takes place when phenolic substrates are utilized.

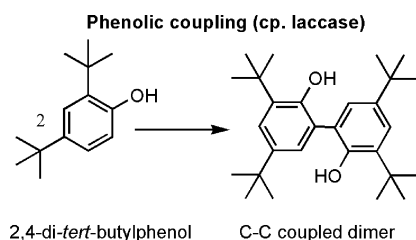


**Fig. 8** Radical carbon-carbon dimerization reaction of 2,4-di-*tert*-butylphenol.

In the literature many examples of copper catalysed polymerisations of phenols have been reported.<sup>49-51</sup> The polymerisation of 2,6-di-*tert*-butylphenol *via* C-O coupling and C-C coupling on the *para*-position was first reported in 1959.<sup>52</sup> In a later stage several copper complexes have been tested in this polymerisation reaction. A Cu(II) bipyridine complex was shown to afford a C-O coupled polymer (MW 13 kDa) and a small amount (5%) of the C-C coupled dimer. In a proposed mechanism for the oxidative phenol polymerization,<sup>48</sup> the rate-determining step is electron transfer from a coordinated phenolate to Cu(II) to give a phenoxy radical and Cu(I); the former is released to react with other radicals, while the latter is reoxidized to Cu(II) by dioxygen. This mechanism could also apply to **1b**, in which the copper-dioxygen complex can react with phenols to form radical coupled products. In the present research we hoped to suppress this type of oxidative polymerisation, because we expected a host-guest complex to be formed, in which the phenolic hydroxyl groups of the substrates (*e.g.* resorcinol) would interact by H-bonds with the carbonyl moieties of the receptor, and thereby be directed away from the reactive copper site. From the results we obtained with 2,4-di-*tert*-butylphenol, we can

conclude, however, that oxidative polymerization does take place in the presence of **1b**. Both the *ortho*- and *para*-positions of the phenolic substrates (*e.g.* resorcinol) are susceptible to coupling, and therefore both oligomers and polymers can be formed.

With the test substrate (2,4-di-*tert*-butylphenol) we observed catalytic C-C coupling of a phenolic substrate to give the dimer with a TON of 10. 2,4-Di-*tert*-butylphenol has no additional reactive *ortho*- or *para*-positions, so that the reactions stops at the dimer stage. No C-O coupling was detected for this substrate, in contrast to what has been observed for 2,6-di-*tert*-butylphenol. Reports in the literature also describe only C-C coupling with the substrate 2,4-di-*tert*-butylphenol.<sup>53,54</sup> The reason for this difference in reactivity between the 2,4- and 2,6-substituted substrates is not discussed in the literature. Based on the literature reported above it is possible that both C-C coupling and C-O coupling take place when phenolic compounds (*e.g.* resorcinol) are used as substrates, and that the reaction proceeds by the same mechanism as discussed above.<sup>48</sup> We are forced to conclude that radical formation and dimerization/polymerization interferes with the intended aromatic and benzylic oxygenation.

**Catalysis by copper(II) complexes of receptors 1 and 2.** Catechol oxidase catalyses the oxidation of catechol to quinone and this reaction is identical to the second step in the catalytic cycle of tyrosinase. The crystal structure of catechol oxidase has been reported.<sup>6,7</sup> The oxidation of 3,5-di-*tert*-butylcatechol (DTBC) to 3,5-di-*tert*-butylquinone (DTBQ) is catalysed by a pair of Cu(II) ions, which are reduced during this reaction (Fig. 9).<sup>55</sup> The resulting Cu(I)<sub>2</sub> complex is reoxidised to Cu(II)<sub>2</sub> by dioxygen; no details on the interaction of O<sub>2</sub> and Cu in this reaction are known. Dinuclear Cu(II) complexes of a number of pyridine-containing ligands<sup>56,57</sup> have also been found to oxidize DTBC with TONs of around 30.

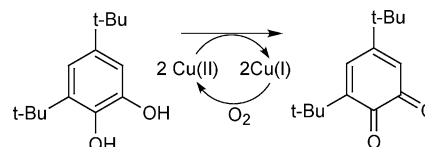


**Fig. 9** Catalytic oxidation of DTBC to DTBQ with Cu ions and O<sub>2</sub>.

The oxidation of 3,5-di-*tert*-butylcatechol (DTBC) to 3,5-di-*tert*-butylquinone (DTBQ) was tested using the Cu(II) complexes of receptors **1** and **2**. These complexes were prepared *in situ* by mixing one equivalent of the appropriate receptor with two equivalents of Cu(II) acetate monohydrate in a 1 : 1 (v/v) solvent mixture of CHCl<sub>3</sub> and MeOH. The reactions were carried out at room temperature and as a control experiment the effect of Cu(II) acetate monohydrate on the oxidation of DTBC in the absence of a receptor was determined. The progress of the

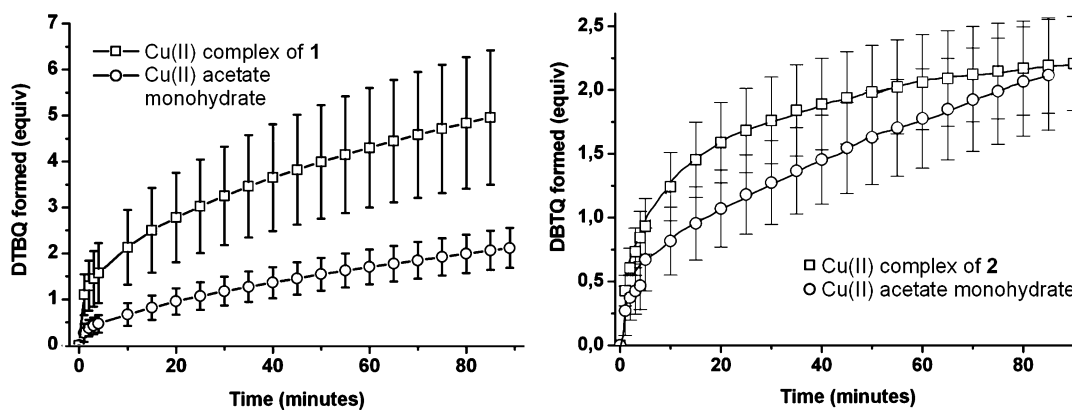


**Fig. 10** Catalytic oxidation of 50 equivalents of DTBC using the Cu(II) complexes of **1** (left) and **2** (right), using Cu(II) acetate as control experiments, as monitored by the change in absorbance at 400 nm. Each reaction was carried out in triplicate (*cf.* error bars).

oxidation reaction was recorded by following the appearance of a distinct UV-vis absorption band of DTBQ at 400 nm ( $\epsilon = 17402 \text{ M}^{-1} \text{ cm}^{-1}$ ) in time. In an experiment where 50 equivalents of substrate was added in one portion, the conversion after 80 min was found to be about twice as high for the copper(II) complex of **1** than for the control reaction (Fig. 10, left), and the difference in initial rate, 1.47 vs. 0.27 equivalents of DTBQ  $\text{min}^{-1}$ , was even larger. The copper(II) complex of **1** thus displays catalytic oxidative activity of 3,5-di-*tert*-butylcatechol, and the rate enhancement compared to the control could be due to substrate binding that can occur in receptor **1**. For the Cu(II) complex of receptor **2**, the extent of the conversion after 80 min is the same as for the control reaction (Fig. 10, right), but the initial rate is approx. two times higher (0.43 vs. 0.27 equivalents of DTBQ  $\text{min}^{-1}$ ).

Several explanations can be given for the relatively high initial reaction rate of the Cu(II) complexes of **1** and **2** compared to the subsequent slow phase. Apparently, the initial reaction of the Cu(II) to the Cu(I) complexes (and of DTBC to DTBQ) is fast, but the reoxidation to the Cu(II) complex is slow. Such biphasic kinetics or “burst kinetics” has been observed before for supramolecular catalysts, for example in the case of the ester hydrolysis by Cu(II) complexes of imidazole-appended cyclophanes, where the catalyst is rapidly acylated but only slowly deacylated.<sup>58</sup> A possible explanation is that the initially fast reaction is slowed down by product inhibition, *i.e.* by binding of the product in the cavity. Another explanation may be the difference in copper ligation: the slow reoxidation of the Cu(I) complexes of the receptors may be due to a difference in redox potentials between the Cu(II)/Cu(I) couples in copper acetate and in the complexes with the pyridine ligands in the receptors. The pyridyl groups have a high tendency to stabilize Cu(I), and this slows down the reoxidation to Cu(II). In order to further study the factors underlying the difference in reactivity between Cu(II) acetate monohydrate and the copper centre in receptor **1**, a test reaction with 1 equivalent of DTBC was carried out, followed by a titration with aliquots of 2 equivalents of DTBC.

Upon addition of 1 equivalent of DTBC, the TON with the Cu(II) complex of receptor **1** reached the expected value of 1 within 15 s. (Fig. 11, squares). The absorption at 400 nm continued to rise even after that, which can be partly explained by interference of the LMCT band of the Cu(I) pyridyl complex with the DTBQ band at 400 nm; the  $\epsilon$  at  $\lambda_{\text{max}}$  (340 nm) is  $3500 \text{ M}^{-1} \text{ cm}^{-1}$  per Cu (see above) and is estimated to be  $1100 \text{ M}^{-1} \text{ cm}^{-1}$  at 400 nm. After 7 min the absorption of the band at 400 nm (Fig. 11) started to decrease and returned, after approx. 20 min, to the level corresponding to the formation of approx. one equivalent of DTBQ. From this we can conclude that the initial oxidation resulting in stoichiometric conversion is fast but that the reoxidation of the catalyst from Cu(I) to

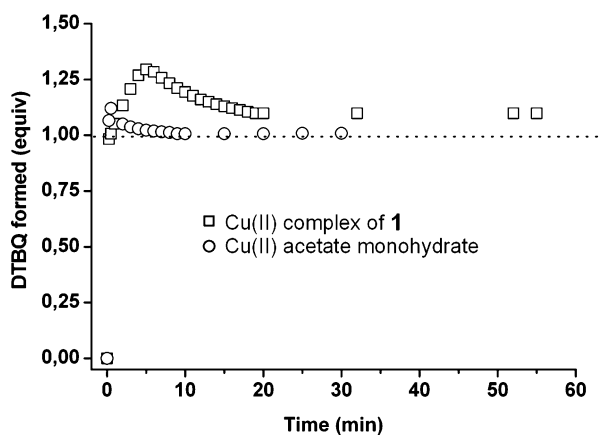


**Fig. 11** Stoichiometric conversion of DTBC catalysed by Cu(II) acetate (open circles) and the dinuclear Cu(II) complex of receptor **1** (open squares) as monitored by the change in absorbance at 400 nm.

Cu(II) is the rate limiting step for catalytic turnover by the Cu(II) complex of **1**. Compared to **1**, the reoxidation of Cu(I) acetate monohydrate (Fig. 11, circles) is fast. The titration with DTBC was continued by adding 4 aliquots of 2 equivalents of substrate each to the reaction mixture already containing 1 equivalent of substrate and 1 equivalent of either Cu(II) acetate or  $\frac{1}{2}$  equivalent of the Cu(II) complex of **1** (this equals 1 equivalent of Cu(II) in **1**). The aliquots were added every 4 h and after 16 h a total of 9 equivalents of substrate had been added.

As can be seen in Table 5, the percentages of conversion and initial rates are stable for Cu(II) acetate during the titration, but gradually decrease for the Cu(II) complex of receptor **1**. The most straightforward explanation for this result is that the Cu(II) complex of **1** decreases in catalytic efficiency because it decomposes with time. It should be noted, however, that even the initial rate of the catalysis by the Cu(II) complex of **1** is slightly slower than that of Cu(II) acetate in the titration experiments, whereas it was significantly higher in the experiment with a large excess of substrate (50 equivalents, see above). This indicates that the catalytic activity of the Cu(II) complex of **1** is sensitive to inhibition by the product DTBQ, which is more effective when the substrate DTBC is not present in large excess; this is also an alternative explanation for the observation that the apparent activity of the Cu(II) complex of **1** decreases as the product DTBQ accumulates during the titration.

**Catalysis by the Fe(II) complex of 2.** In addition to the well-known heme enzymes, non-heme biocatalysts are often found in Nature. An important example is the Fe(II) complex of the glycopeptide bleomycin which catalyses the degradation of

**Table 5** DTBC conversion and initial rate of reaction, catalyzed by Cu(II) acetate and the dinuclear Cu(II) complex of receptor **1**

Aliquot	— <sup>a</sup>	First	Second	Third	Fourth
Equiv. added	1	2	2	2	2
Total equiv. (cumulative)	1	3	5	7	9
Cu(II) complex of <b>1</b>					
Initial rate (slope)	4.0	1.8	0.8	0.8	0.3
TON at 80 min	1.0	2.0	1.7	1.7	~1.4
Conversion (%)	100	100	85	85	~70
Cu(II) acetate					
Initial rate (slope)	4.2	5.7	5.0	5.0	5.4
TON at 80 min	1.0	1.6	1.6	1.6	1.7
Conversion (%)	100	80	80	80	85

<sup>a</sup> The progress curve of the addition of the first equivalent of substrate is graphically presented in Fig. 11.

DNA by oxidative cleavage and is clinically used in cancer treatment.<sup>59</sup> Five nitrogen donors from the ligand surround the Fe(II) ion, while one coordination position is available for dioxygen to bind.<sup>60</sup> Activated bleomycin (ABLM) [Fe(III)BLM(OOH)] is formed by the reaction of the Fe(II) complex of BLM with dioxygen and a one-electron reductor like ascorbate. Besides DNA cleavage BLM also oxidises olefinic substrates with iodosobenzene, dioxygen or peroxides as the oxidant.<sup>61</sup> Synthetic models of non-heme biocatalysts include the Fe(III) complex of TPA (**7a**), which oxidizes cyclohexene to cyclohexanol (TON 3) and cyclohexane (TON 0.7).<sup>62</sup> Recently, the Fe(II) complex of another ligand **11** (N3PY) has been reported (Chart 4), which coordinates to iron with three pyridyl ligands and one amine nitrogen, in a fashion similar to TPA. The oxidation of cyclooctene with **11**-Fe(II) and hydrogen peroxide (50 equivalents) proceeds with TONs of 14 and 19 for *cis*-oxide and *cis*-diol, respectively.<sup>63</sup> TPA shows a TON of 2–3 for both the epoxide and the *cis*-diol when 10 equivalents of hydrogen peroxide are used.<sup>64</sup>

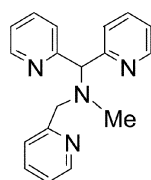
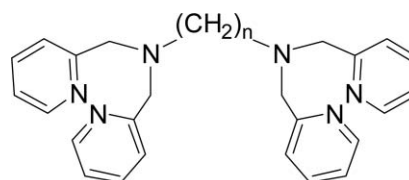
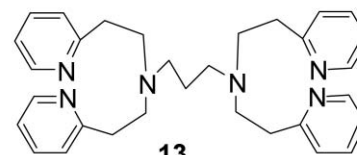
**11**, N3PY

Chart 4

In order to study its epoxidation reactivity towards alkenes, a Fe(II) complex of receptor **2** was prepared *in situ* using acetonitrile as the solvent (0.44 mM). The formation of this complex as [2·(Fe(II)<sub>2</sub>)]<sup>4+</sup> with perchlorate counterions was confirmed by electrospray mass spectrometry (see ESI†). To a solution of the complex in CH<sub>2</sub>Cl<sub>2</sub>, 1000 equivalents of cyclooctene and 50 equivalents of hydrogen peroxide were added. The reactivity was measured after 1 h by means of GC analysis of the reaction mixture.<sup>61–63</sup> Unfortunately, the complex did not show any reactivity towards the substrate. As a first step towards the study of substrates that might be included in the cavity of **2** in chlorinated solvents, the oxidation of cyclooctene by the Fe(II) complex of **2** was studied in dichloromethane. As water would interfere with the hydrogen bonding interactions, by which the target substrates are supposed to be bound in the receptor, the urea adduct of hydrogen peroxide was used as the oxidant instead of aqueous hydrogen peroxide. This experiment proved to be difficult due to the lack of solubility of the Fe(II) complex

of **2** in this solvent. Therefore, the reactivity of a suspension was tested but no changes in colour or any reactivity were observed.

**Catalysis by the Mn(III) complex of 1.** Reactivity found for synthetic dinuclear manganese complexes<sup>65,66</sup> comprises for example epoxidation<sup>67</sup> and alcohol oxidation.<sup>68</sup> The dinuclear Mn(III) complex of 1,4,7-trimethyl-1,4,7-triazacyclononane (**9b**)<sup>69</sup> is an active epoxidation catalyst with a TON of 400 for styrene,<sup>70,71</sup> but turned out to be too strong an oxidant for practical purposes, causing fabric damage when applied as a bleaching agent in a laundry detergent.<sup>72</sup> When hydrogen peroxide is used as the oxidant in epoxidation reactions it is essential that the catalase activity of the manganese complexes is suppressed. This can be achieved by (i) working in acetone as a solvent, which most probably leads to the formation of a perhydrate species ((CH<sub>3</sub>)<sub>2</sub>C(OH)(OOH)),<sup>73</sup> or (ii) by addition of co-catalysts, such as oxalate or ascorbic acid.<sup>67,74</sup> Homolytic cleavage of hydrogen peroxide leads to radicals that can cause unselective side reactions, which can be minimized by tuning the ligand and oxidation conditions.<sup>75</sup> Recently, a new type of binucleating ligand has been developed for the epoxidation of alkenes using manganese complexes.<sup>76</sup> Two bis(2-methylpyridine)amine units were linked together using different spacers, giving *N,N,N',N'*-tetrakis((pyridin-2-yl)methyl)ethane-1,2-diamine (**12a**) and *N,N,N',N'*-tetrakis((pyridin-2-yl)methyl)propane-1,3-diamine (**12b**) (Chart 5). It was found that the length of the spacer is determining for the catalytic activity, since the ethylene-bridged ligand **12a** is unreactive in epoxidation catalysis, whereas the propylene-bridged ligand **12b** is active with a TON up to 582 for epoxidation of cyclohexene after 4 h.<sup>77</sup>

**12a**, n = 2  
**12b**, n = 3**13**  
Chart 5

The oxidation of primary alcohols to the corresponding aldehydes is one of the key reactions in organic chemistry.<sup>78</sup> It can be carried out by metal complexes with dioxygen or hydrogen peroxide as the oxidant. Manganese complexes of **9b** are also active in the oxidation of benzyl alcohols using H<sub>2</sub>O<sub>2</sub> with a TON ranging from 80 to 1000.<sup>66</sup> The bis(2-methylpyridine)amine-based ligands described above have also been tested in alcohol oxidation.<sup>79</sup> The *in situ* prepared Mn catalyst based on ligand **12b** displays a TON of 293 for benzyl alcohol after 4 h, while the complex based on **12a** is not active.<sup>79</sup>

Epoxidation of alkenes was tested using Mn(III) complexes of receptor **1** as catalysts following a literature procedure.<sup>67,78</sup> The catalyst solutions were prepared *in situ* from 0.1 mol% of the Mn(III) complex of receptor **1** and 8 equivalents of hydrogen peroxide (relative to the substrate). Cyclooctene was used as a test substrate, with cyclooctene oxide and *cis*- and *trans*-1,2-cyclooctanediol as possible products. Both mono- and dinuclear Mn(III) complexes of receptor **1** were tested and both were found to be inactive in epoxidation, since no products were observed. In a second set of experiments, alcohol oxidation was studied using three different substrates, *viz.* benzyl alcohol, *p*-methylbenzyl alcohol and 3,5-dihydroxybenzyl alcohol, and a 1 mM solution of either a mononuclear or a dinuclear Mn(II) complex of receptor **1**. No formation of products was observed.

Mn(III) catalysts that are normally used for epoxidation catalysis are based on two bis(2-methylpyridine)amine units linked by a spacer of appropriate length (**12b**) (Chart 5). In our case, the basket can be regarded as a special type of spacer that has the capacity of binding the substrate. However, the metal binding ligands in receptor **1** are bis(2-ethylpyridine)amines, containing one extra methylene groups in between the pyridyl group and the amino function. This gives rise to a different coordination geometry (or no complexation at all) and could account for the lack of reactivity of receptor **1** as compared to **12b**. This hypothesis can be easily tested by comparing a ligand that contains methylpyridyl groups with a ligand that contains ethylpyridyl groups. Ligand **12b** meets the former requirements, while for the latter **13** (*N,N,N',N'*-tetrakis(pyridin-2-yl)methyl)propane-1,3-diamine) was designed. No epoxidation activity was observed with the Mn(III) complex of **13** for any of the substrates tested (cyclohexene, cyclooctene, *trans*-2-octene, *trans*-4-octene, 1-decene, cinnamyl alcohol), while **12b** was reactive.<sup>77</sup> From these results it can be concluded that bis(2-ethylpyridine) units such as present in **1** are not suitable as ligands of Mn(III) in epoxidation reactions.

## Conclusions

PY2-appended receptor **1** and TPA-appended receptor **2** have been studied with low-temperature UV-vis spectroscopy and X-ray absorption spectroscopy. Furthermore, a new dual type setup<sup>24</sup> for both XAS and UV-vis experiments has been introduced that allowed the correlation of different spectroscopic data on one and the same oxygenated sample.

The dinuclear copper(I) complex of receptor **1** is capable of binding dioxygen at  $-80\text{ }^{\circ}\text{C}$  to form the  $\mu\text{-}\eta^2\text{:}\eta^2\text{ Cu}_2\text{O}_2$  complex **1b**, as confirmed by both UV-vis and EXAFS experiments. Complex **1b** was found to be only stable at  $-80\text{ }^{\circ}\text{C}$  and warming up to higher temperatures resulted in a break down of the copper dioxygen complex, however not in decomposition of the receptor **1** itself. It was established by UV-vis that complex **1b** was stable at  $-80\text{ }^{\circ}\text{C}$  during vacuum and/or argon purging, and hence dioxygen is bound irreversibly. A dioxygen titration confirmed that the stoichiometry of **1b** was 2 Cu per O<sub>2</sub>. Studies of the dependence of the rate of dioxygen binding on the concentration of **1a** revealed that this binding is intramolecular and not intermolecular, *i.e.* one molecule of dioxygen is bound by the two copper ions of one receptor molecule. The rate of dioxygen binding to **1a** is proportional to the dioxygen bubbling frequency.

XANES studies revealed that the oxidation state of **1a** was Cu(I) and that of **1b** Cu(II) and that consistent results on oxygenated samples are obtained with the new type of XAS cell<sup>24</sup> than with the old type of cell.<sup>12</sup> EXAFS studies showed that the structure of **1b** contains an almost flat  $\mu\text{-}\eta^2\text{:}\eta^2\text{ Cu}_2\text{O}_2$  moiety.

The presence of 30 vol.% of acetonitrile in THF turned out to effectively inhibit the oxygenation of **1a** to **1b**, probably due to coordination of a molecule of acetonitrile to the copper centre. This was concluded from the lack of features characteristic of oxygenation in the UV-vis, XANES and EXAFS spectra.

UV-vis experiments on the copper complexes **2a** and **2b** revealed that the copper centre is oxidized as concluded from the loss of the Cu(I) band but that no new Cu(II) complex is formed, at least not one that can be attributed to a known copper dioxygen complex. Thus no formation of a either a  $\mu\text{-}\eta^2\text{:}\eta^2$ , bis- $\mu\text{-oxo}$  or *trans*- $\mu\text{-1,2}$  complex could be confirmed.

XANES experiments revealed a characteristic Cu(I) edge for **2a** with a prominent pre-edge transition, in addition to a significant shift of the edge to higher energy upon oxygenation, consistent with the oxidation of Cu(I) to Cu(II) and confirming the results of the UV-vis experiments. EXAFS showed that at most two of the three pyridyl groups of a TPA unit coordinate to copper, in line with earlier NMR results.<sup>8</sup>

Catalytic oxidation studies with various transition metals have been carried out using metal complexes of receptors **1** and **2**. It was found that receptor **2** is only active as its Cu(II) complex in the catalytic oxidation of DTBC to DTBQ. It has been found earlier that the dinuclear Cu(I) complex of receptor **2** can bind one of its ligand pyridyl arms in the substrate binding cavity.<sup>8</sup> This inclusion phenomenon was not tested for the complexes of the other metals used in this work but it is likely that it will occur as well. This inclusion may be the reason for the lack of reactivity of receptor **2** for most reactions tested.

The Cu(I)<sub>2</sub>O<sub>2</sub> complex of receptor **1** is active in the radical C–C coupling of 2,4-di-*tert*-butylphenol and shows a TON of 10 for the formation of the dimeric product. This result also provides evidence for the presence of a radical oxidation process in the reactions with other phenolic substrates. No oxygenation activity towards the ligand itself or toward exogenous ligands was observed for the copper dioxygen complex of receptor **1**. This lack of oxygenation is the result of the fact that radical coupling reactions prevail.

This radical coupling also leads to the formation of oligomeric and polymeric products in the case of substrates containing the 3,5-dihydroxybenzene moiety. The formation of these polymeric products is due to the same reaction as the formation of the dimer of 2,4-di-*tert*-butylphenol. The coupling reaction takes place at the *ortho*- and *para*-positions and in the case of 2,4-di-*tert*-butylphenol only one of these position is available and hence dimers are the only product formed. In the case of 3,5-dihydroxybenzene substrates more positions are available for coupling, leading to the formation of polymeric structures. This reaction prevents any oxygen insertion in the phenolic substrate. Comparing our results with those of the biological systems mentioned in the introduction section, *i.e.* galactose oxidase, dopamine- $\beta$ -hydroxylase, tyrosinase, catechol oxidase, and laccase, we conclude that of our model systems, the Cu(II) complex of **2** displays catechol oxidase activity, whereas the catalytic activity of **1b** most resembles that of laccase.

No reactivity was observed in the case of the Mn(III) complexes of receptor **1**, in epoxidation nor in alcohol oxidation. This was found to be due to the structure of the receptor, since in model reactions ligands with bis(2-ethylpyridine)amine units were found to be unreactive in contrast to ligands with bis(2-methylpyridine)amine units.

Furthermore, no reactivity was observed for the Fe(II) complexes of receptor **2**, which is probably due to solubility problems.

## Acknowledgements

The authors thank Jan Hanss (EMBL) for assistance with the XAS in an early stage of the project. We acknowledge the Dutch Research Council (NWO) for support through its chemical branch (CW, formerly SON) with a grant in the Supramolecular Technology programme (to M. C. F., R. J. M. N., B. L. F.), and the European Community for support in the framework of the Access to Research Infrastructure Action of the improving Human Potential programme to the EMBL Hamburg Outstation, Contract No. HPRI-CT-1999-00017. K. D. K. is grateful for financial support from the National Institutes of Health (USA), GM28962. B. L. F. acknowledges financial support from the Ministry of Economic Affairs through the ECOX programme.

## References

- 1 K. A. Magnus, B. Hazes, H. Tonthat, C. Bonaventura, J. Bonaventura and W. G. J. Hol, *Proteins: Struct. Funct. Genet.*, 1994, **19**, 302–309.
- 2 A. Volbeda and W. G. J. Hol, *J. Mol. Biol.*, 1989, **209**, 249–279.
- 3 M. E. Cuff, K. I. Miller, K. E. van Holde and W. A. Hendrickson, *J. Mol. Biol.*, 1998, **278**, 855–870.
- 4 G. L. Woolery, L. Powers, M. Winkler, E. I. Solomon, K. Lerch and T. G. Spiro, *Biochim. Biophys. Acta*, 1984, **788**, 155–161.
- 5 E. I. Solomon, U. M. Sundaram and T. E. Machonkin, *Chem. Rev.*, 1996, **96**, 2563–2605.
- 6 T. Klabunde, C. Eicken, J. C. Saccettini and B. Krebs, *Nat. Struct. Biol.*, 1998, **5**, 1084–1090.
- 7 C. Gerdemann, C. Eicken and B. Krebs, *Acc. Chem. Res.*, 2002, **35**, 183–191.
- 8 V. S. I. Sprakel, M. C. Feiters, J. A. A. W. Elemans, B. Lucchese, K. D. Karlin and R. J. M. Nolte, *Eur. J. Org. Chem.*, submitted.
- 9 C. F. Martens, R. J. M. Klein Gebbink, M. C. Feiters and R. J. M. Nolte, *J. Am. Chem. Soc.*, 1994, **116**, 5667–5670.
- 10 R. J. M. Klein Gebbink, C. F. Martens, M. C. Feiters and R. J. M. Nolte, *Chem. Commun.*, 1997, 389–390.
- 11 R. J. M. Klein Gebbink, C. F. Martens, P. J. A. Kenis, R. J. Jansen, H.-F. Nolting, V. A. Solé, M. C. Feiters, K. D. Karlin and R. J. M. Nolte, *Inorg. Chem.*, 1999, **38**, 5755–5768.
- 12 M. C. Feiters, R. J. M. Klein Gebbink, V. A. Solé, H.-F. Nolting, K. D. Karlin and R. J. M. Nolte, *Inorg. Chem.*, 1999, **38**, 6171–6180.
- 13 K. D. Karlin, Z. Tyeklar, A. Farooq, M. S. Haka, P. Gosh, R. W. Cruse, Y. Gultneh, J. C. Hayes, P. J. Toscano and J. Zubieta, *Inorg. Chem.*, 1992, **31**, 1436–1451.
- 14 K. D. Karlin and A. D. Zuberbühler, *Bioinorganic Catalysis*, ed. J. Reedijk and E. Bouwman, 2nd edn., 1999, pp. 469–534.
- 15 M. L. Baldwin, D. E. Root, J. E. Pate, K. Fujisawa, N. Kitajima and E. I. Solomon, *J. Am. Chem. Soc.*, 1992, **114**, 10421–10431.
- 16 N. Kitajima, K. Fujisawa, Y. Moro-oka and K. Toriumi, *J. Am. Chem. Soc.*, 1989, **111**, 8975–8976.
- 17 N. Kitajima, K. Fujisawa, C. Fujimoto, U. Muro-oka, S. Hashimoto, T. Kitagawa, K. Toriumi, K. Tatsumi and A. Nakamura, *J. Am. Chem. Soc.*, 1992, **114**, 1277–1291.
- 18 R. R. Jacobson, Z. Tyeklar, A. Farooq, K. D. Karlin, S. Liu and J. Zubieta, *J. Am. Chem. Soc.*, 1988, **110**, 3690–3692.
- 19 K. D. Karlin, J. C. Hayes, Y. Gultneh, R. W. Cruse, J. W. McKown, J. P. Hutchinson and J. Zubieta, *J. Am. Chem. Soc.*, 1984, **106**, 2121–2128.
- 20 C. X. Zhang, H.-C. Liang, E.-I. Kim, Q.-F. Gan, Z. Tyeklar, K.-C. Lam, A. L. Rheingold, S. Kaderli, A. D. Zuberbühler and K. D. Karlin, *Chem. Commun.*, 2001, 631–632.
- 21 H. V. Obias, Y. Lin, N. N. Murthy, E. Pidcock, E. I. Solomon, M. Ralle, N. J. Blackburn, Y.-M. Neuhold, A. D. Zuberbühler and K. D. Karlin, *J. Am. Chem. Soc.*, 1998, **120**, 12960–12961.
- 22 S. Itoh, H. Kumei, M. Taki, S. Nagatomo, T. Kitagawa and S. Fukuzumi, *J. Am. Chem. Soc.*, 2001, **123**, 6708–6709.
- 23 L. Santagostini, M. Gullotti, E. Monzani, L. Casella, R. Dillinger and F. Tuzcek, *Chem. Eur. J.*, 2000, **6**, 519–522.
- 24 V. S. I. Sprakel, M. C. Feiters, R. J. M. Nolte, P. M. F. M. Hombergen, A. Groenen and H. J. R. De Haas, *Rev. Sci. Instrum.*, 2002, **73**, 2994–2998.
- 25 R. J. M. Klein Gebbink, A. W. Bosman, M. C. Feiters, E. W. Meijer and R. J. M. Nolte, *Chem. Eur. J.*, 1999, **5**, 65–69.
- 26 R. J. M. Klein Gebbink, *Supramolecular Metallobiosite Analogues*, PhD Thesis, University of Nijmegen, 1998.
- 27 P. L. Holland, C. J. Cramer, E. C. Wilkinson, S. Mahapatra, K. R. Rodgers, S. Itoh, M. Taki, S. Fukuzumi, L. Que, Jr. and W. B. Tolman, *J. Am. Chem. Soc.*, 2000, **122**, 792–802.
- 28 S. Mahapatra, J. A. Halfen, E. C. Wilkinson, G. F. Pan, C. J. Cramer, L. Que, Jr. and W. B. Tolman, *J. Am. Chem. Soc.*, 1995, **117**, 8865–8866.
- 29 S. Mahapatra, J. A. Halfen, E. C. Wilkinson, G. F. Pan, X. Wang, V. G. Young, Jr., C. J. Cramer, L. Que, Jr. and W. B. Tolman, *J. Am. Chem. Soc.*, 1996, **118**, 11555–11574.
- 30 S. Mahapatra, S. Kaderli, A. Llobet, Y.-M. Neuhold, T. Palanché, J. A. Halfen, V. G. Young, Jr., T. A. Kaden, L. Que, Jr., A. D. Zuberbühler and W. B. Tolman, *Inorg. Chem.*, 1997, **36**, 6343–6356.
- 31 J. Cahoy, P. L. Holland and W. B. Tolman, *Inorg. Chem.*, 1999, **38**, 2161–2168.
- 32 Y. Gultneh, B. Ahvazi, A. R. Khan, R. J. Butcher and J. P. Tuchagues, *Inorg. Chem.*, 1995, **34**, 3644–3645.
- 33 K. D. Karlin, N. Wei, B. Jung, S. Kaderli, P. Niklaus and A. D. Zuberbühler, *J. Am. Chem. Soc.*, 1993, **115**, 9506–9514.
- 34 K. D. Karlin, S. Kaderli and A. D. Zuberbühler, *Acc. Chem. Res.*, 1997, **30**, 139–147.
- 35 B. Lucchese, K. J. Humphreys, D.-H. Lee, C. D. Incarvito, R. D. Sommer, A. L. Rheingold, and K. D. Karlin, *Inorg. Chem.*, 2003, **43**, 5987–5998.
- 36 B. Lucchese, PhD Dissertation, 2004, The Johns Hopkins University, Baltimore, MD, USA.
- 37 L.-S. Kau, D. J. Spira-Solomon, J. E. Penner-Hahn, K. O. Hodgson and E. I. Solomon, *J. Am. Chem. Soc.*, 1987, **109**, 6433–6442.
- 38 A. Volbeda, M. C. Feiters, M. G. Vincent, E. Bouwman, B. Dobson, K. H. Kalk, J. Reedijk and W. G. J. Hol, *Eur. J. Biochem.*, 1989, **181**, 669–673.
- 39 M. Schatz, M. Becker, F. Thaler, F. Hampel, S. Schindler, R. R. Jacobson, Z. Tyeklar, N. N. Murthy, P. Ghosh, Q. Chen, J. Zubieta and K. D. Karlin, *Inorg. Chem.*, 2001, **40**, 2312–2322.
- 40 Z. Tyeklar, R. R. Jacobson, N. Wei, N. N. Murthy, J. Zubieta and K. D. Karlin, *J. Am. Chem. Soc.*, 1993, **115**, 2677–2689.
- 41 N. J. Blackburn, R. W. Strange, A. Farooq, M. S. Haka and K. D. Karlin, *J. Am. Chem. Soc.*, 1988, **110**, 4263–4272.
- 42 K. D. Karlin, M. S. Haka, R. W. Cruse, G. J. Meyer, A. Farooq, Y. Gultneh, J. C. Hayes and J. Zubieta, *J. Am. Chem. Soc.*, 1988, **110**, 1196–1207.
- 43 D.-H. Lee, N. Wei, N. N. Murthy, Z. Tyeklar, K. D. Karlin, S. Kaderli, B. Jung and A. D. Zuberbühler, *J. Am. Chem. Soc.*, 1995, **117**, 12498–12513.
- 44 C. F. Martens, R. P. Sijbesma, R. J. M. Klein Gebbink and R. J. M. Nolte, *Recl. Trav. Chim. Pays-Bas*, 1993, **112**, 400–403.
- 45 R. P. Sijbesma and R. J. M. Nolte, *J. Org. Chem.*, 1991, **56**, 3122–3124.
- 46 H. K. A. C. Coolen, J. A. M. Meeuwis, P. W. N. M. van Leeuwen and R. J. M. Nolte, *J. Am. Chem. Soc.*, 1995, **117**, 11906–11913.
- 47 R. F. Stewart and L. L. Miller, *J. Am. Chem. Soc.*, 1980, **102**, 4999–5004.
- 48 E. Tsuchida, K. Yamamoto, *Bioinorganic Catalysis*, ed. J. Reedijk, Marcel Dekker, New York, 1993, pp. 29–87.
- 49 P. G. Aubel, S. S. Khokhar, W. L. Driessen, G. Challa and J. Reedijk, *J. Mol. Catal. A: Chem.*, 2001, **175**, 27–31.
- 50 H. Higashimura, M. Kubota, A. Shiga, K. Fujisawa, Y. Moro-oka, H. Uyama and S. Kobayashi, *Macromolecules*, 2000, **33**, 1986–1995.
- 51 P. J. Baesjou, W. L. Driessen, G. Challa and J. Reedijk, *J. Mol. Catal. A: Chem.*, 1998, **135**, 273–283.
- 52 A. S. Hay, H. S. Stafford, G. F. Endres and J. W. Eustance, *J. Am. Chem. Soc.*, 1959, **81**, 6335–6336.
- 53 M. Taki, S. Teramae, S. Nagatomo, Y. Tachi, Y. Kitagawa, S. Itoh and S. Fukuzumi, *J. Am. Chem. Soc.*, 2002, **124**, 6367–6377.
- 54 V. Mahadevan, M. J. Henson, E. I. Solomon and T. D. P. Stack, *J. Am. Chem. Soc.*, 2000, **122**, 10249–10250.
- 55 J. Ackerman, F. Meyer, E. Kaifer and H. Pritzkow, *Chem. Eur. J.*, 2002, **8**, 247–258.
- 56 A. Neves, L. M. Rossi, A. J. Bortoluzzi, B. Szpoganicz, C. Wiezbicki and E. Schwingel, *Inorg. Chem.*, 2002, **41**, 1788–1794.
- 57 P. Gentschev, N. Möller and B. Krebs, *Inorg. Chim. Acta*, 2000, **300–302**, 442–452.
- 58 Y. Murakami, Y. Aoyama and M. Kida, *J. Chem. Soc., Perkin Trans. 2*, 1980, 1665.
- 59 R. M. Burger, *Chem. Rev.*, 1998, **98**, 1153–1169.
- 60 T. E. Lehman, L.-J. Ming, M. E. Rosen and L. Que, Jr., *Biochemistry*, 1997, **36**, 2807–2816.
- 61 N. Murugesan and S. M. Hecht, *J. Am. Chem. Soc.*, 1985, **107**, 493–500.
- 62 C. Kim, K. Chen, J. Kim and L. Que, Jr., *J. Am. Chem. Soc.*, 1997, **119**, 5964–5965.
- 63 M. Klopstra, G. Roelfes, R. Hage, R. M. Kellogg and B. L. Feringa, *Eur. J. Inorg. Chem.*, 2004, 846.
- 64 K. Chen and L. Que, Jr., *Angew. Chem., Int. Ed.*, 1999, **38**, 2227–2229.

- 65 R. Noyori, M. Aoki, and K. Sato, *Chem. Commun.*, 2003, 1977–1986.
- 66 T. Katsuki, *Chem. Soc. Rev.*, 2004, **33**, 437–444.
- 67 J. Brinksma, L. Schmieder, G. van Vliet, R. Boaron, R. Hage, D. E. de Vos, P. L. Alsters and B. L. Feringa, *Tetrahedron Lett.*, 2002, **43**, 2619–2622.
- 68 C. Zondervan, R. Hage and B. L. Feringa, *Chem. Commun.*, 1997, 419–420.
- 69 K. Wieghardt, U. Bossek, D. Ventur and J. Weiss, *J. Chem. Soc., Chem. Commun.*, 1985, 347–349.
- 70 W.-C. Cheng, W.-H. Fung and C.-M. Che, *J. Mol. Catal. A: Chem.*, 1996, **113**, 311–319.
- 71 V. C. Quee-Smith, L. Delpizzo, S. H. Jureller, J. L. Kerschner and R. Hage, *Inorg. Chem.*, 1996, **35**, 6461–6455.
- 72 M. Verrall, *Nature*, 1994, **369**, 511.
- 73 D. E. de Vos and T. Bein, *Chem. Commun.*, 1996, 917–918.
- 74 D. E. de Vos, B. F. Sels, M. Reynaers, Y. V. Subba Rao and P. A. Jacobs, *Tetrahedron Lett.*, 1998, **39**, 3221–3224.
- 75 B. Meunier, *Chem. Rev.*, 1992, **92**, 1411–1456.
- 76 J. Brinksma, R. Hage, J. Kerschner and B. L. Feringa, *Chem. Commun.*, 2000, 537–538.
- 77 J. Brinksma, *Manganese Catalysts in Homogeneous Oxidation Catalysis*, PhD thesis, University of Groningen, 2002.
- 78 R. A. Sheldon, J. K. Kochi, in *Metal-Catalysed Oxidations of Organic Compounds*, Academic Press, New York, 1981.
- 79 J. Brinksma, M. T. Rispens, R. Hage and B. L. Feringa, *Inorg. Chim. Acta*, 2002, **337**, 75–82.